



Optimization of adsorption of Cr(VI) from aqueous solution by *Leucaena leucocephala* seed shell activated carbon using design of experiment

Adeyinka S. Yusuff¹

Received: 11 April 2018 / Accepted: 10 October 2018 / Published online: 22 November 2018
© The Author(s) 2018

Abstract

The activated carbon from *Leucaena leucocephala* seed shell was prepared by chemical activation, characterized and used as adsorbent for the removal of hexavalent chromium [Cr(VI)] from aqueous solution via batch mode adsorption. The variables affecting the adsorption process, initial adsorbate concentration, pH, adsorbent dosage and temperature were optimized using central composite design (CCD) of the response surface methodology (RSM) at fixed contact time of 60 min. Equilibrium adsorption isotherm and kinetic were also studied. The analysis of variance (ANOVA) revealed that all the variables studied had significant effects on the removal efficiency of Cr(VI). The obtained data showed that 71.49 mg/L initial Cr(VI) concentration, 4.22 solution pH, 0.57 g adsorbent dosage and 26.2 °C temperature resulted in 95.62% adsorption. Equilibrium adsorption isotherm and kinetic studies showed that Freundlich isotherm and pseudo-second-order kinetic model fitted well to the experimental data. The activated carbon from *Leucaena leucocephala* seed shell was found to be efficient for Cr(VI) adsorption.

Keywords Activated carbon · Hexavalent chromium · Characterization · Kinetic · Isotherm

Introduction

Indiscriminate release of industrial wastewater containing heavy metals into water bodies is of great concern. Larger amount of effluent which contains dissolved heavy metals and other inorganic contaminants is being released by many industries, and it is a known fact that most of the dissolved heavy metals are poisonous and non-biodegradable and tend to easily find their way into food chain, thus affecting negatively both plants and animals (Mohammed-Ridha et al. 2017; Vasudevan and Lakshmi 2011). One of the heavy metals often found in industrial wastewater is chromium. However, some of the industries that discharge wastewater containing chromium include fertilizer, electroplating, mining processing, metal processing, tanning, paints, battery and domestic plumbing materials (Sing et al. 2006;

Argun et al. 2007; Kamaraj et al. 2015). Chromium exists in two different elemental states, that is, hexavalent chromium [Cr(VI)] and trivalent chromium [Cr(III)]. Research has proven that Cr(VI) is much more poisonous than Cr(III) (Gorzin and Abadi 2017). Direct exposure to Cr(VI) can lead to lungs cancer, epigastria pain, vomiting and chronic diarrhea (Vasudevan and Lakshmi 2011). Due to the negative effects of chromium, World Health Organization (WHO) has set a maximum permissible concentration for chromium in drinking water to be 0.05 mg/L (Vasudevan and Lakshmi 2011). Thus, there is need to properly treat industrial effluent prior to it discharge into environment.

The most commonly used techniques for removing chromium from water/wastewater include chemical precipitation, ion exchange, electrocoagulation, reverse osmosis, membrane separation, electro-Fenton process, nanofiltration and adsorption (Matlock et al. 2001; Inglezakis et al. 2007; Nurbas Nourbakhsh et al. 2002; Rahmani et al. 2015; Mnif et al. 2017; Gorzin and Abadi 2017). Among these methods, adsorption is found to be effective, eco-friendly, less expensive and simple. Thus, it is adopted as usual purification process in various industries (Lim and Lee 2015). Adsorption is a unit operation that deals with separation

✉ Adeyinka S. Yusuff
yusuffas@abuad.edu.ng

¹ Department of Chemical and Petroleum Engineering,
College of Engineering, Afe Babalola University, Ado-Ekiti,
Nigeria

of contaminants from liquid or gaseous mixture by using porous solid material called adsorbent.

In recent time, rapid removal of Cr(VI) from water/wastewater has been proven to be possible by activated carbon-based adsorbents. Nowadays research is therefore focused on derivation of adsorbents from carbon-based materials such as coconut tree sawdust (Selvi et al. 2001), walnut shell (Derdour et al. 2018), hazelnut shell (Kobyta 2004), peanut shell (Al-Othman et al. 2012), paper mill sludge (Gorzin and Abadi 2017), Luffa sponge (Wang et al. 2016), corn cob (Murugesan et al. 2013), *Delonix regia* pods (Renuga et al. 2010), bamboo waste (Dula et al. 2014) and melon husk (Akpan et al. 2015). Another carbonaceous material which can serve as a potential starting ingredient for an adsorbent is *Leucaena leucocephala* seed shell.

Leucaena leucocephala is a small fast-growing leguminous tree which belongs to a family of *Fabaceae*, and it is commonly known as white lead tree (El feel and Elmagboul 2016). The plant as shown in Fig. 1a consists of flowers, narrowly oblong leaves, stem, seeds and pods (shells). Its flower possesses head which is round and white with pit balls of many hairy, pale yellow anthers. The plant has small, flat, green leaves as well as green bean pods which turn brown when dry as can be seen in Fig. 1b. Contained in the pods are bead necklace-like row of seeds. The seeds are flat, oval, a rich glossy brown color. In Nigeria, *L. leucocephala* is found everywhere and regarded as a weed. Many of its seeds and shells are waste in the environment and are rich source of charcoal/activated carbon. However, if adequate attention is given to the white lead tree plant, it can successfully be a continuous source of activated carbon for wastewater purification. This is because it grows annually and is available in abundance.

As reflected in the literature, few successful experiments have been conducted on the use of adsorbents

derived from *L. leucocephala* seed shells to remove heavy metals from aqueous environment; thus, adequate experimental data have not been really provided. In the present work, the prepared activated carbon from *L. leucocephala* seed shells was studied as a low-cost adsorbent for removing Cr(VI) from aqueous solutions, and the LLAC adsorbent was characterized by Brunauer–Emmett–Teller (BET), X-ray diffraction (XRD), scanning electron microscopy (SEM) and Fourier transform infrared (FTIR) techniques in order to gain insight into its physical, chemical and surface morphological properties. Statistical optimization of variables affecting the adsorption process was conducted using central composite design (CCD) of response surface methodology (RSM) in design expert. Moreover, equilibrium adsorption isotherm and kinetics studies were investigated.

Materials and method

Materials

The *L. leucocephala* seed shells were handpicked under its tree situated behind Owolabi hall, Afe Babalola University, Ado-Ekiti, Nigeria. All the chemical compounds used in this study, including potassium heptaoxidochromate ($K_2Cr_2O_7$), sodium hydroxide (NaOH) and sulfuric acid (H_2SO_4) (BDH, England), were of analytical grade procured from Topjay Chemical Enterprise, Ado-Ekiti, Nigeria. A 1000 mg/L stock solution of Cr(VI) was prepared by dissolving 2.83 g of $K_2Cr_2O_7$ in 1000 mL of deionized water. Various solutions of needed initial Cr(VI) concentrations were obtained by diluting the stock solution with required amount of deionized water.

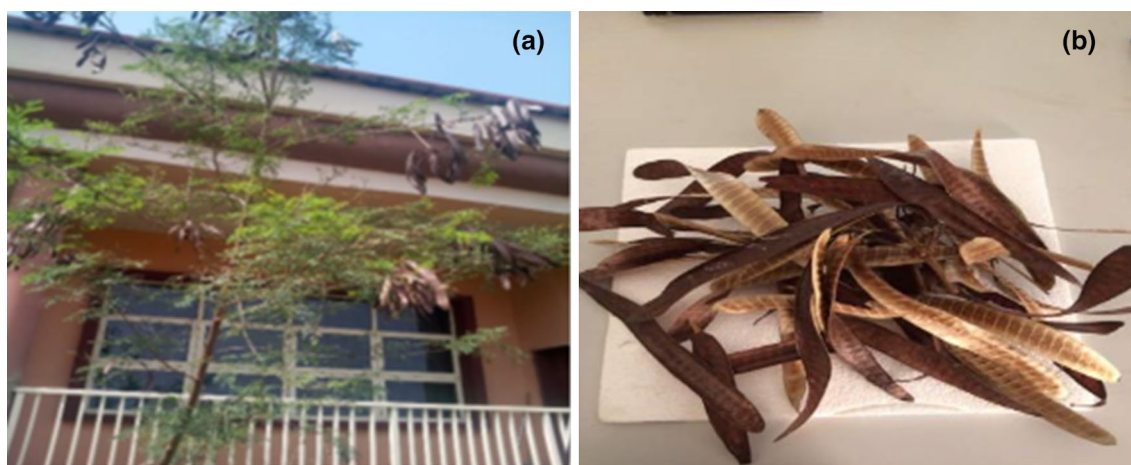


Fig. 1 a *Leucaena leucocephala* tree and b *Leucaena leucocephala* seed shells

Preparation of adsorbent

The collected shells were opened up to remove the seeds contained in them and thoroughly washed by distilled water to remove dust and other impurities. It was thereafter heated up at 105 °C for 24 h in an oven. The dried shells were crushed into smaller pieces by mortar and pestle and ground into powder with the aid of mechanical grinder. The obtained powder was sieved to a particle size of 150 μm. In order to activate the obtained powder, 30 g of the powder was soaked in 50 mL of 1.5 M NaOH solution and left overnight for proper impregnation. The impregnate was heated up at 60 °C for 24 h in an oven. The raw sample was thereafter carbonized at 550 °C for 2 h in a muffle furnace. The obtained *L. leucocephala* seed shells based on activated carbon sample will be referred as LLAC.

Characterization of adsorbent

The textural properties of the prepared LLAC which include BET surface area and pore size distributions were determined using Quantachrome analyzer (Nova station A, version 11.03, USA) based on the principle of adsorption/desorption of nitrogen at 77 K and 60/60 s (ads/des) equilibrium time. X-ray diffraction (XRD) was used to confirm the structural characteristics and unique fingerprints of the LLAC sample, which was conducted on a Rigaku D/Max-III C XRD (PW 1800) analyzer. A Cu-κ α radiation (1.54051 Å) was employed to generate diffraction patterns at ambient temperature in the scanning angle 2θ of 5°–90°. In addition, the LLAC crystallite size was determined using Scherrer’s expression which is given in Eq. 1.

$$d = \frac{0.9\lambda}{\beta \cos \theta} \tag{1}$$

where *d* is the crystallite size of the active phase (nm), λ is the X-ray wavelength, θ is the angle of diffraction and β is the full width at half maximum of the peak.

Scanning electron microscopy (SEM-JEOL-JSM 7600F) was used to determine the surface morphology, crystalline structure and orientation of the LLAC sample, while the surface functional groups on LLAC sample before and after adsorption of Cr(VI) were determined by Fourier transform

infrared (FTIR) spectrophotometer (IR Affinity 1S, Shimadzu, Japan).

Experimental design and statistical analysis

In the current study, central composite design (CCD), which is an optimization tool contained in RSM, was used for examining the influence of some variables on adsorption process. In order to determine the optimum conditions, four process independent variables were chosen: initial Cr(VI) concentration, *C* mg/L, solution pH, *p*, adsorbent dosage, *d* g and temperature, *T* °C, and their effects on the removal efficiency of Cr(VI) were evaluated. A total of 30 experimental runs were conducted in this work, 2⁴ = 16 cube points, 6 replications at the center point and 8 axial points. The obtained experimental data were analyzed using Design expert 7.0.0 software. The experimental ranges and the level of the chosen input variables for Cr(VI) removal efficiency (*R*) are presented in Table 1.

The main objective of this work is to determine the optimum conditions for adsorption of Cr(VI) from aqueous environment onto LLAC. However, the removal efficiency (*R*) which is the response was determined via batch adsorption experiment and also used to develop a mathematical model. The model correlates the dependent variables (*R*) to the four independent variables considered through second-order polynomial response equation according to Eq. 2.

$$R = b + b_C C + b_p p + b_d d + b_T T + b_{Cp} Cp + b_{Cd} Cd + b_{CT} CT + b_{pd} pd + b_{pT} pT + b_{dT} dT + b_{CC} C^2 + b_{pp} p^2 + b_{dd} d^2 + b_{TT} T^2 \tag{2}$$

where *R* is the response variable of Cr(VI) removal efficiency. The *b* is the constant term; *b_i*s are the regression coefficients for linear terms; *b_{ik}* are the regression coefficients for quadratic terms; and *C*, *p*, *d* and *T* represent coded experimental level of the variables.

Batch adsorption studies

The adsorption activities of the LLAC were conducted in a set of each 250-mL conical flasks containing 50 mL of the required concentration of an adjusted pH of Cr(VI) solution. The flasks were covered and agitated in a

Table 1 Levels of the adsorption process parameters considered

| Description | Variable | Unit | Level | | | | |
|------------------------------|----------|------|-------|-----|-----|-----|-------|
| | | | −2 | −1 | 0 | +1 | +2 |
| Initial Cr(VI) concentration | <i>C</i> | mg/L | 8.58 | 50 | 150 | 250 | 29.42 |
| Solution pH | <i>p</i> | – | 2.76 | 4 | 7 | 10 | 11.24 |
| Adsorbent dosage | <i>d</i> | g | 0.03 | 0.2 | 0.6 | 1.0 | 1.17 |
| Temperature | <i>T</i> | °C | 20.86 | 25 | 35 | 45 | 49.14 |

temperature-controlled water bath shaker (SearchTech Instrument) operating at a constant stirring speed of 150 rpm. The process was conducted according to the experimental conditions obtained with experimental design (Table 1) at fixed contact time of 60 min. Upon equilibrium attainment, each sample was centrifuged at high speed for 10 min and decanted. The concentration of un-adsorbed Cr(VI) was thereafter analyzed by atomic absorption spectrophotometer (AAS, Buck Scientific 210VGP, USA). The Cr(VI) removal efficiency, $R(\%)$ and amount of Cr(VI) adsorbed at equilibrium, q_e , mg/g, were determined as follows:

$$R, \% = \frac{(C_o - C_e)}{C_o} \times 100\% \quad (3)$$

$$q_e = \frac{(C_o - C_e)V}{w} \quad (4)$$

where C_o and C_e (mg/L) are the initial and equilibrium concentrations of Cr(VI) in aqueous solution, V (L) is the volume of the Cr(VI) solution and w (g) is the weight of the LLAC sample used.

Equilibrium adsorption isotherm

In this study, the applicability of two-parameter isotherm models (Langmuir and Freundlich) was tested in order to choose the most appropriate model that would best describe and predict the adsorption of Cr(VI) onto LLAC.

Langmuir isotherm

The nonlinear form of Langmuir adsorption isotherm model is expressed as follows:

$$q_e = \frac{q_{\max} b C_e}{(1 + b C_e)} \quad (5)$$

where q_e (mg/g) is the amount of Cr(VI) adsorbed at equilibrium, C_e (mg/L) is the equilibrium concentration of Cr(VI) in aqueous solution, q_{\max} (mg/g) is the maximum adsorption capacity and b is the Langmuir equilibrium constant.

The most important features of the Langmuir model can be described as dimensionless quantity called separation factor (R_L) whose value determines the nature of the adsorption isotherm whether it is favorable ($0 < R_L < 1$), unfavorable ($R_L > 1$), irreversible ($R_L = 0$) or linear ($R_L = 1$). It can be determined using Eq. 6:

$$R_L = \frac{1}{(1 + b C_o)} \quad (6)$$

where C_o (mg/L) is the maximum initial Cr(VI) concentration and b (L/mg) is the Langmuir equilibrium constant.

Freundlich isotherm

The Freundlich isotherm is the oldest known two-parameter adsorption model which is applied for multilayer, heterogeneous adsorption sites and is expressed as (Freundlich 1906).

$$q_e = k_F C_e^{1/n} \quad (7)$$

where C_e (mg/L) is the equilibrium concentration of Cr(VI) in solution, k_F [mg/g(L/mg)^{1/n}] indicates the adsorption capacity of the adsorbent and n is an adsorption intensity.

Kinetic modeling

Pseudo-first-order and pseudo-second-order kinetic models were employed to evaluate the acquired experimental data to gain insight into controlling mechanism of the adsorption of Cr(VI) on LLAC. The linearized forms of the pseudo-first-order (Lagergren 1898) and pseudo-second-order (Ho and McKay 1998) models are expressed in Eqs. (8) and (9), respectively, as follows:

$$\log(q_e - q_t) = \log q_e - \frac{k_1 t}{2.303} \quad (8)$$

$$\frac{t}{q_t} = \frac{1}{k_2 q_e^2} + \frac{t}{q_e} \quad (9)$$

where q_e (mg/g) is the amount of Cr(VI) adsorbed at equilibrium, q_t is the amount of Cr(VI) adsorbed at time t (mg/g) and k_1 (min⁻¹) and k_2 (g mg⁻¹min⁻¹) are pseudo-first-order and pseudo-second-order rate constants, respectively.

Results and discussions

Characterization of LLAC

The textural properties of the prepared adsorbent before and after loading of Cr(VI) ions were determined, and the

Table 2 Textural properties of prepared LLAC adsorbent before and after adsorption

| Sample | BET surface area (m ² /g) | Total pore volume (cm ³ /g) |
|-------------------------|--------------------------------------|--|
| LLCA | 89.74 | 0.02320 |
| LLAC loaded with Cr(VI) | 6.39 | 0.00056 |

results obtained are presented in Table 2. The BET surface area of the prepared activated carbon without Cr(VI) was $89.74 \text{ m}^2/\text{g}$ compared to activated carbon ($68.4 \text{ m}^2/\text{g}$) reported by Alias et al. (2017). However, the surface area of LLAC loaded with Cr(VI) ions was observed to be largely reduced. In addition, there was a significant decrease in total pore volume of the adsorbent after the adsorption of Cr(VI) onto its surface as can be seen in Table 2. This observation is attributed to aggregation of adsorption sites indicative of the complete loading of Cr(VI) ions onto the surface of LLAC sample used (Lim and Lee 2015). This is corroborated by SEM and FTIR analyses.

The crystalline phases present in the prepared sample of LLAC were examined by XRD analysis. Figure 2 depicts the XRD diffraction pattern of prepared activated carbon. The XRD patterns exhibited well-defined peaks related to the crystalline phase of carbon. The three peaks detected at $2\theta = 15.2^\circ$ (not shown in the spectrum), 23.8° and 28.6° were attributed to the crystallite graphitic structure (Sugashini

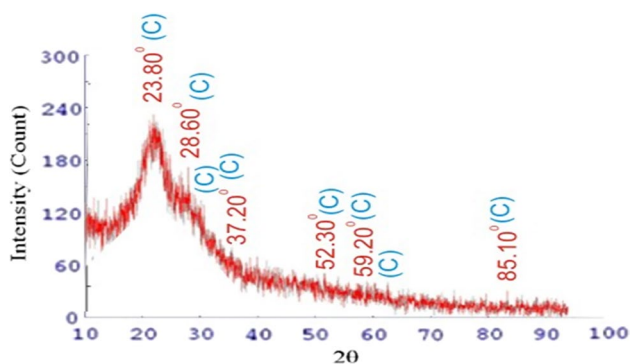


Fig. 2 XRD diffraction patterns of LLAC

and Begum 2015; Girgis et al. 2007). Generally, a noticeable hump in the range $20\text{--}30^\circ$ represents a significant degree of disorder, typical of carbon structure. A similar observation was reported for activated carbon synthesized from olive stones (Bohli et al. 2015) and Malawian baobab fruit shells (Vunain et al. 2017). Additionally, the average crystallite size of the prepared LLAC sample studied, which was determined by Scherrer equation (Eq. 1) was 2.94 \AA .

The surface morphology of LLAC sample before and after adsorption was examined by SEM analysis, and the results are depicted in Fig. 3. Figure 3a shows the SEM image of LLAC sample without Cr(VI) which was taken at a magnification of $9000\times$ and a scale bar of $10 \mu\text{m}$, respectively. The image revealed various pores on the surface of the sample studied, which indicate a good possibility for Cr(VI) to be adsorbed. However, the SEM image of LLAC loaded with Cr(VI) shown in Fig. 3b revealed that those pores earlier seen on the fresh adsorbent have been blocked due to adsorption of Cr(VI) onto its surface.

In order to evaluate the mechanism of the adsorption of Cr(VI) and also identify the functional groups present on the surface of prepared activated carbon (LLAC), FTIR analysis was performed. The FTIR spectra of LLAC before and after adsorption of Cr(VI) are depicted in Fig. 4 and Table 3. Some peaks were shifted and disappeared, and new ones were developed. The new peak observed at 941.29 cm^{-1} is attributed to the Cr=O bond of CrO_7^{2-} on the LLAC (Oyedoh and Ekwonu 2016). In addition, a change in intensity and shift of the carbonyl stretching band (C=O) from 1681.96 to 1631.83 cm^{-1} is a result of contact between the chromium solution and LLAC. Table 3 reveals that most of the surface functional groups present on the LLAC adsorbent include saturated aliphatic (C–H), unsaturated aliphatic (C=C and C≡C), alcoholic (C–O–H) and

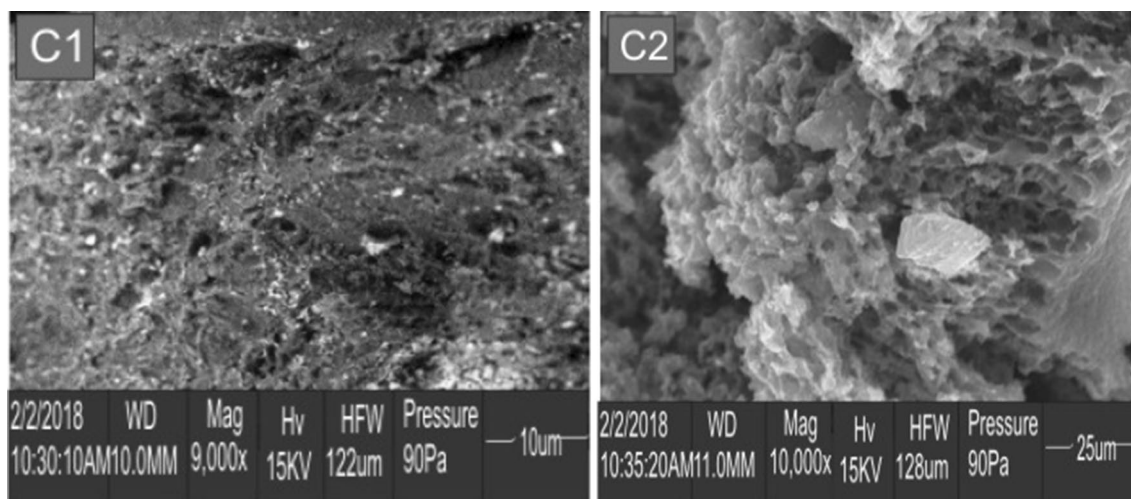


Fig. 3 SEM images of LLAC adsorbent a before and b after loading of Cr(VI)

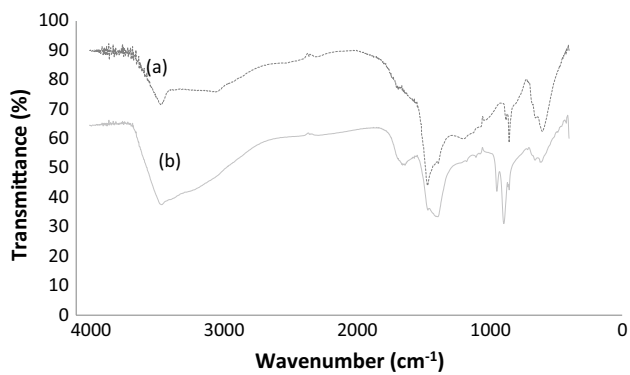


Fig. 4 FTIR spectra of LLAC **a** before and **b** after loading of Cr(VI)

O–H), carboxylic (C–O and C=O), carbonyl (C=O) and amine (C–N) bonds. However, the presence of all these functional groups is responsible for the effective performance of LLAC during adsorption process.

Central composite design (CCD) model and data analysis

The 4-factor CCD matrix as generated by the software and the experimental data obtained in the batch adsorption of Cr(VI) by LLAC are presented in Table 4.

As suggested by the CCD, a quadratic model which correlates a response (removal efficiency) and the independent variables was chosen and expressed by the second-order polynomial equation in terms of coded factors after removing the insignificant model terms as follows:

$$R = 77.31 - 8.03C - 5.15p + 5.93d - 2.43T + 3.19Cd + 2.52pd - 1.95p^2 - 3.63d^2 + 2.88T^2 \quad (10)$$

The removal efficiencies (%) of Cr(VI) have been predicted by Eq. (3) and are presented in Table 4. In general, there were agreements between the experimental and predicted values of Cr(VI) removal efficiency. The linear correlation (R^2) which was used to evaluate the correlation between the actual and predicted responses was obtained from the developed model to be 0.9697. This indicates that 96.97% of the variation for percentage removal of Cr(VI) are described by the variables studied and also indicates that only 3.03% of variation does not describe by the model. Furthermore, the model adequacy was also examined by analysis of variance (ANOVA). Table 5 depicts the results of the quadratic response surface model fitting in the form of ANOVA. According to Giwa et al. (2012), ANOVA subdivides the complete variation of the results into variation associated with the model and the one associated with experimental errors, indicating whether the variation from the model is significant or not. This evaluation is performed by F -value, which is the ratio of model mean square to the residual error. A model is said to be a good predictor of the experimental data, if F -value obtained is evidently greater than the tabulated F -value (Giwa et al. 2012; Ani et al. 2015). The F -value obtained herein was 34.32, thus indicating the fitness of the model.

More so, the probability of error value ($\text{Prob} > F$) was employed to evaluate the significance of each of the model terms. However, values of $\text{Prob} > F$ less than 0.0500

Table 3 FTIR bands of LLAC adsorbent

| Band | Wave number (cm ⁻¹) | | Assignment/vibration |
|------|---------------------------------|----------------------|---|
| | Before Cr(VI) loading | After Cr(VI) loading | |
| 1 | 3460.41; 3055.35 | 3456.55; 3242.45 | O–H stretching vibration in absorbed water |
| 2 | – | 2918.40 | Two bands for –CH ₂ – stretching |
| 3 | 2521.05 | – | C ≡ C stretching |
| 4 | 2289.58 | 2337.80 | C–O stretching |
| 5 | – | 2079.33 | C=O stretching |
| 6 | 1681.96 | 1631.83 | C=O stretching |
| 7 | – | 1560.46 | C=C stretching |
| 8 | 1462.09 | 1458.23 | CH ₃ antisym deformation |
| 9 | 1383.01 | 1383.01 | C–CH ₃ sym deformation |
| 10 | 1192.05 | 1215.19 | C–O stretching |
| 11 | – | 1168.90 | C–N stretching |
| 12 | 1118.75 | 1097.53 | C–O stretching |
| 13 | 1024.24 | – | C–O–H stretching |
| 14 | – | 941.29 | Cr–O bond of chromate anion |
| 15 | 871.85; 848.71 | 889.21; 848.71 | CH out-of-plane deformation |
| 16 | 651.96; 599.88 | 653.89; 607.60 | C–O–H twist |
| 17 | – | 484.15 | Out-of-plane ring bending |

Table 4 Batch mode adsorption process parameters in coded and actual values with Cr(VI) removal efficiencies (responses) from experimental results

| Run no. | Batch adsorption process variables | | | | Cr(VI) removal efficiency, <i>R</i> (%) | |
|---------|---|--------------|--------------------------------|----------------------------|---|--------------------|
| | Initial Cr(VI) concentration, <i>C</i> (mg/L) | pH, <i>p</i> | Adsorbent dosage, <i>d</i> (g) | Temperature, <i>T</i> (°C) | Predicted value | Experimental value |
| 1 | 50 (- 1) | 4 (- 1) | 0.2 (- 1) | 25 (- 1) | 91.37 | 89.47 |
| 17 | 250 (+ 1) | 4 (- 1) | 0.2 (- 1) | 25 (- 1) | 71.28 | 72.89 |
| 4 | 50 (- 1) | 10 (+ 1) | 0.2 (- 1) | 25 (- 1) | 76.53 | 78.85 |
| 7 | 250 (+ 1) | 10 (+ 1) | 0.2 (- 1) | 25 (- 1) | 51.59 | 49.42 |
| 11 | 50 (- 1) | 4 (- 1) | 1.0 (+ 1) | 25 (- 1) | 89.48 | 90.61 |
| 13 | 250 (+ 1) | 4 (- 1) | 1.0 (+ 1) | 25 (- 1) | 82.15 | 81.32 |
| 14 | 50 (- 1) | 10 (+ 1) | 1.0 (+ 1) | 25 (- 1) | 84.71 | 81.78 |
| 10 | 250 (+ 1) | 10 (+ 1) | 1.0 (+ 1) | 25 (- 1) | 72.53 | 73.96 |
| 22 | 50 (- 1) | 4 (- 1) | 0.2 (- 1) | 45 (+ 1) | 82.17 | 82.71 |
| 18 | 250 (+ 1) | 4 (- 1) | 0.2 (- 1) | 45 (+ 1) | 62.21 | 63.87 |
| 29 | 50 (- 1) | 10 (+ 1) | 0.2 (- 1) | 45 (+ 1) | 71.20 | 70.76 |
| 25 | 250 (+ 1) | 10 (+ 1) | 0.2 (- 1) | 45 (+ 1) | 46.39 | 47.22 |
| 3 | 50 (- 1) | 4 (- 1) | 1.0 (+ 1) | 45 (+ 1) | 84.97 | 85.86 |
| 24 | 250 (+ 1) | 4 (- 1) | 1.0 (+ 1) | 45 (+ 1) | 77.77 | 77.42 |
| 6 | 50 (- 1) | 10 (+) | 1.0 (+ 1) | 45 (+ 1) | 84.07 | 84.42 |
| 15 | 250 (+ 1) | 10 (+ 1) | 1.0 (+ 1) | 45 (+ 1) | 72.02 | 72.65 |
| 28 | 8.58 (- 2) | 7 (0) | 0.6 (0) | 35 (0) | 89.51 | 89.83 |
| 8 | 291.42 (+ 2) | 7 (0) | 0.6 (0) | 35 (0) | 66.79 | 65.09 |
| 16 | 150 (0) | 2.76 (- 2) | 0.6 (0) | 35 (0) | 80.69 | 79.03 |
| 12 | 150 (0) | 11.24 (+ 2) | 0.6 (0) | 35 (0) | 66.13 | 66.41 |
| 9 | 150 (0) | 7 (0) | 0.03 (- 2) | 35 (0) | 61.65 | 60.21 |
| 26 | 150 (0) | 7 (0) | 1.17(+ 2) | 35 (0) | 86.50 | 78.5 |
| 19 | 150 (0) | 7 (0) | 0.6 (0) | 20.86 (- 2) | 79.63 | 87.73 |
| 20 | 150 (0) | 7 (0) | 0.6 (0) | 49.14 (+ 2) | 77.31 | 77.02 |
| 30 | 150 (0) | 7 (0) | 0.6 (0) | 35 (0) | 77.31 | 73.91 |
| 2 | 150 (0) | 7 (0) | 0.6 (0) | 35 (0) | 77.31 | 81.09 |
| 5 | 150 (0) | 7 (0) | 0.6 (0) | 35 (0) | 77.31 | 75.89 |
| 23 | 150 (0) | 7 (0) | 0.6 (0) | 35 (0) | 77.31 | 76.02 |
| 21 | 150 (0) | 7 (0) | 0.6 (0) | 35 (0) | 77.31 | 81.66 |
| 27 | 150 (0) | 7 (0) | 0.6 (0) | 35 (0) | 77.31 | 78.02 |

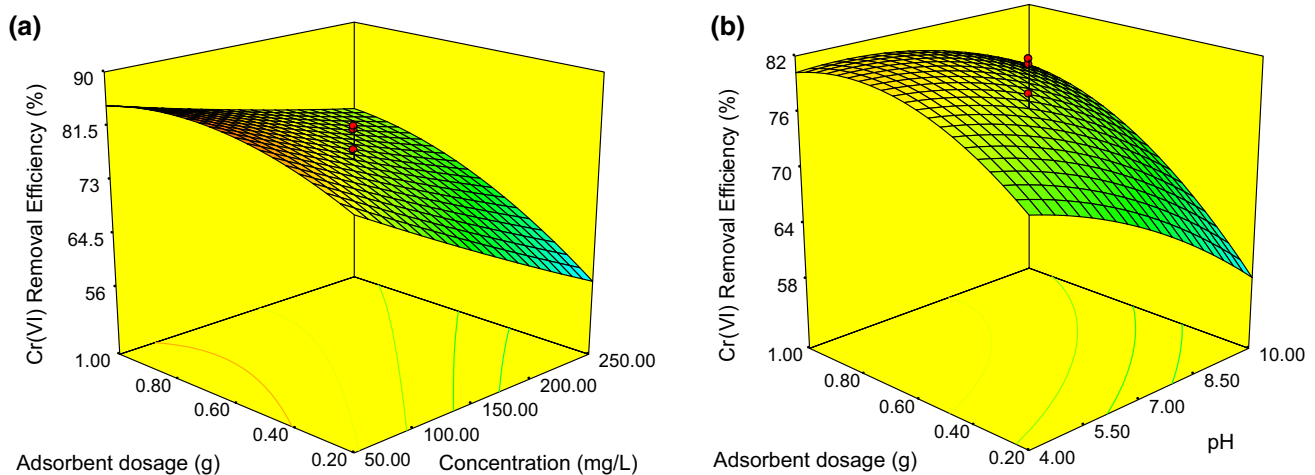
indicate terms are significant. In this current study, *C*, *p*, *d*, *T*, *Cd*, *pd*, *p*², *d*² and *T*² were significant model terms, while *Cp*, *CT*, *pT*, *dT* and *C*² were insignificant terms for removal efficiency of Cr(VI). Based on the *F*-value (Table 5), the four process variable studied had significant influence on the Cr(VI) removal efficiency. The initial Cr(VI) concentration (*C*) showed the largest *F*-value of 194.74, indicating that it had the most significant effect on the adsorption of Cr(VI), compared to pH (*p*), adsorbent dosage (*d*) and temperature (*T*). Meanwhile, only quadratic effects of pH, adsorbent dosage (*d*) and temperature on removal efficiency of Cr(VI) were significant. As also contained in Table 5, the lack of fit *F*-value of 0.8082 indicates the lack of fit is not significant relative to the

pure error. However, nonsignificant lack of fit is good as it gears the model toward perfect fitness.

Figure 5a depicts the 3D surface plot of Cr(VI) removal efficiency as a function of initial Cr(VI) concentration (*C*) and adsorbent dosage (*d*). It was observed that there was sharp improvement in Cr(VI) removal efficiency with increasing adsorbent dosage. The probable reason is that when the adsorbent dose is increased, the active sites of LLAC are increased, which could adsorb more Cr(VI) ions; thus, removal efficiency increases. The higher removal efficiencies of Cr(VI) at higher adsorbent dosages were also attributed to the fact that the adsorption sites on the LLAC remained unsaturated during Cr(VI) removal from aqueous solution (Gorzin and Abadi 2017). This observation is in

Table 5 Analysis of variance (ANOVA) for fit of Cr(VI) removal efficiency from central composite design

| Source | Sum of squares | df | Mean square | F-value | Prob > F | Remark |
|---------------------------------------|----------------|----|-------------|---------|----------|----------------|
| Model | 3185.56 | 14 | 227.54 | 34.32 | <0.0001 | Significant |
| <i>C</i> | 1291.19 | 1 | 1291.19 | 194.74 | <0.0001 | Significant |
| <i>p</i> | 529.81 | 1 | 529.81 | 79.91 | <0.0001 | Significant |
| <i>d</i> | 704.44 | 1 | 704.44 | 106.24 | <0.0001 | Significant |
| <i>T</i> | 117.79 | 1 | 117.79 | 17.76 | 0.0008 | Significant |
| <i>Cd</i> | 163.01 | 1 | 163.01 | 24.59 | 0.0002 | Significant |
| <i>pd</i> | 101.46 | 1 | 101.46 | 15.30 | 0.0014 | Significant |
| <i>p</i> ² | 35.42 | 1 | 35.42 | 5.34 | 0.0354 | Significant |
| <i>d</i> ² | 123.02 | 1 | 123.02 | 18.55 | 0.0006 | Significant |
| <i>T</i> ² | 77.39 | 1 | 77.39 | 11.67 | 0.0038 | Significant |
| Residual | 99.46 | 15 | 6.63 | | | |
| Lack of fit | 51.74 | 10 | 5.17 | 0.54 | 0.8082 | Nonsignificant |
| Pure error | 47.71 | 5 | 9.54 | | | |
| Cor total | 3285.02 | 29 | | | | |
| $R^2 = 0.9697$; $Adj - R^2 = 0.9415$ | | | | | | |

**Fig. 5** Interactive effect of parameters on the removal efficiency of Cr(VI) **a** concentration versus adsorbent dosage and **b** pH versus adsorbent dosage

trend with most of the studies reported on the combined effects of adsorbent dosage and initial adsorbate concentration (Mohammed-Ridha et al. 2017; Radnia et al. 2012). Figure 5b depicts the 3D surface plot showing the combined effects of pH (*p*) and adsorbent dosage (*d*) on the removal efficiency of Cr(VI) ions (*R*). As can be observed from Fig. 5b, almost 80% of Cr(VI) was adsorbed from aqueous solution with pH of 4.0 when it was treated with 1.0 g LLAC sample. The reason for this observation could be that the affinity of the protons (H^+) on the surface of LLAC improved a binding force between the positively charged LLAC surface and oxy-anion component of the dissolved chromium salt ($Cr_2O_7^{2-}$) (Gupta et al. 2010). Meanwhile, it was revealed by the result obtained that adsorbent dosage highly interacts with other variables. This observation is in

trend with most results reported in the literature (Chiban et al. 2009; Gorzin and Abadi 2017).

Process optimization

The optimum values of the process parameters for the maximum Cr(VI) removal efficiency were determined to be 71.49 mg/L initial Cr(VI) concentration (*C*), 4.22 solution pH (*p*), 0.57 g adsorbent dosage (*d*) and 26.2 °C temperature (*T*). At these optimum conditions, the predicted and experimental removal efficiencies of Cr(VI) from aqueous solution were 91.26 and 95.62%, respectively. After the establishment of the optimum condition for Cr(VI) adsorption onto LLAC, another experimental run was conducted at optimum values of the process

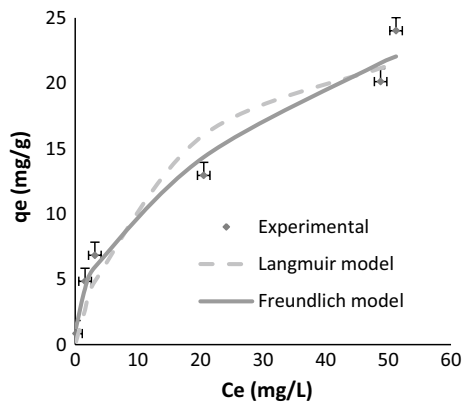


Fig. 6 Two-parameter isotherm models for adsorption of Cr(VI) onto LLAC under optimum conditions (adsorbent dosage = 0.57 g; pH 4.22; temperature = 26.2 °C; and contact time = 60 min)

Table 6 Two-parameter isotherm constants and correlation coefficients for adsorption of Cr(VI) onto LLAC adsorbent

| Isotherm | Value |
|------------------------------------|--------|
| Langmuir | |
| q_{max} (mg/g) | 27.53 |
| b (L/mg) | 0.0681 |
| R^2 | 0.9466 |
| R_L | 0.1703 |
| Freundlich | |
| k_F (mg/g(L/mg) ^{1/n}) | 3.47 |
| n | 2.13 |
| R^2 | 0.9778 |

parameters and the actual removal efficiency of Cr(VI) was obtained. The result obtained herein indicates that there was reasonably agreement between the predicted and experimental Cr(VI) removal efficiencies. This implies that the adopted objective function to optimize the adsorption of Cr(VI) onto LLAC and to determine the maximum Cr(VI) uptake by RSM is successful.

Table 7 Comparison of maximum adsorption capacities of different adsorbents for Cr(VI) removal from aqueous system

| Adsorbent | Maximum adsorption capacity (mg/g) | Temperature, T (°C) | References |
|------------------------------------|------------------------------------|---------------------|----------------------------|
| Paper mill sludge | 23.18 | 45 | Gorzin and Abadi (2017) |
| Peanut shell | 14.31 | 40 | Al-Othman et al. (2012) |
| Walnut shell | 43.12 | 40 | Ghasemi et al. (2015) |
| Natural clinoptilolite zeolite | 10.42 | 24–26 | Jorfi et al. (2017) |
| Rice husk | 62.9 | 35 | Sugashini and Begum (2015) |
| Palm kernel shell | 8.25 | – | Atieh (2011) |
| Sugarcane bagasse | 5.75 | 25 | Garg et al. (2007) |
| Maple sawdust | 5.1 | – | Yu et al. (2003) |
| Teak sawdust | 0.89 | – | Sumathi et al. (2005) |
| <i>L. leucocephala</i> seed shells | 27.53 | 26.2 | Current study |

Adsorption equilibrium isotherm

In testing the applicability of Langmuir and Freundlich isotherms, the Cr(VI) initial concentration employed was from 8.58 to 291.42 mg/L. For both isotherms, the experimental data are plotted as q_e against C_e by nonlinear Eqs. (5) and (7). From Fig. 6 which depicts a comparison of the experimental data with the Langmuir and Freundlich isotherms, the values of the parameters contained in the two isotherm models were determined and are presented in Table 6. However, the applicability of the two isotherms considered was compared using linear correlation coefficient (R^2). The values of R^2 for both isotherms are also presented in Table 6. Based on the values of R^2 , Freundlich isotherm provides the best fit to the adsorption equilibrium data of Cr(VI). This indicates that the adsorption of Cr(VI) by LLAC adsorbent is evidently with multilayer and heterogeneous adsorption sites. A similar observation was reported for adsorption of Cr(VI) from aqueous solution by natural clinoptilolite zeolite (Jorfi et al. 2017) and rice husk (Sugashini and Begum 2015). As can be seen in Table 6 as well, the value of separation factor (R_L) obtained for Cr(VI) was less than one, indicative of favorable adsorption operation, and Langmuir constant (b) which is attributed to the affinity between adsorbate and adsorbent was found to be 0.0681. The magnitude of Freundlich exponent ($n = 2.13$) gives an indication that adsorption of Cr(VI) on LLAC is favorable (Vasudevan and Lakshmi 2011; Ganesan et al. 2013).

In addition, comparing the maximum adsorption capacity (q_{max}) of different adsorbents for Cr(VI) removal from aqueous solutions as shown in Table 7, LLAC is found to possess a maximum adsorption capacity of 27.53 mg/g at optimum temperature of 26.2 °C and this implies that LLAC could be regarded as an effective adsorbent for the removal of Cr(VI) from wastewater/aqueous solution, especially when compared with peanut shell (14.31 mg/g, Al-Othman et al. 2012) and natural clinoptilolite zeolite (10.42 mg/g, Jorfi et al. 2017).

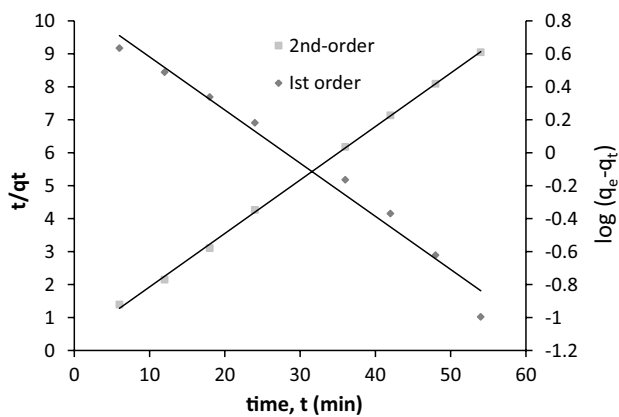


Fig. 7 Pseudo-first-order and pseudo-second-order kinetics for adsorption of Cr(VI) on LLAC [initial Cr(VI) concentration: 71.49 mg/L, pH: 4.22, adsorbent dosage: 0.57, temperature: 26.2 °C and contact time: 60 min]

Table 8 Kinetic model parameters and correlation coefficient obtained for adsorption of Cr(VI) on LLAC under optimum conditions

| Kinetic model | Value of parameter |
|--|--------------------|
| Pseudo-first-order | |
| q_e (exp) (mg/g) | 5.996 |
| q_e (cal) (mg/g) | 2.470 |
| k_1 (min^{-1}) | 0.0744 |
| R^2 | 0.9781 |
| Pseudo-second-order | |
| q_e (cal) (mg/g) | 6.165 |
| k_1 ($\text{g mg}^{-1} \text{min}^{-1}$) | 0.0862 |
| R^2 | 0.9992 |

Adsorption kinetics

The rate of adsorption of Cr(VI) on LLAC was investigated by testing the applicability of two different kinetic models, the pseudo-first-order and pseudo-second-order kinetics. The kinetic parameters of the two models were evaluated from the combined plots of $\log(q_e - q_t)$ against t and t/q_t against t (Fig. 7), and the values of the parameters are presented in Table 8. It is evidently clear that the calculated value of q_e for pseudo-first-order kinetic did not conform to the experimental value of q_e with R^2 value less than that of pseudo-second-order kinetic. This indicates that the acquired experimental data could not be predicted by the pseudo-first-order model. Several researchers reported similar results (Kamaraj et al. 2015; Gorzin and Abadi 2017).

The calculated value of q_e for pseudo-second-order kinetic agreed reasonably well with the experimental value as can be seen in Table 8. This result indicates that the adsorption of Cr(VI) on LLAC was favorably predicted by the pseudo-second-order kinetic. Furthermore, better prediction of the

adsorption of Cr(VI) on LLAC by pseudo-second-order kinetic model indicates that two-phase reaction is involved. During the first phase of the reaction, adsorption occurs rapidly for a short period, whereas adsorption occurs slowly for a long period at second phase. According to Sugashini and Begum (2015), the fast reaction may be due to chemisorption involving electron sharing between the Cr(VI) ions and LLAC. The slow reaction is as a result of mass transfer of Cr(VI) ions to the surface of the LLAC (Hameed et al. 2009; Jun et al. 2009).

Conclusion

The optimization of Cr(VI) adsorption from aqueous solution by the prepared activated carbon showed that the initial Cr(VI) concentration, pH, adsorbent dosage and temperature had significant influence on removal efficiency of Cr(VI). As revealed by RSM, the interaction among the variables studied enhanced the adsorption of Cr(VI). At the following optimum conditions: 71.49 mg/L initial Cr(VI) concentration, 4.22 solution pH, 0.57 g adsorbent dosage and 26.2 °C temperature, the maximum Cr(VI) uptake of 95.62% was obtained. Freundlich isotherm provided the best fit to the experimental data, indicating that the adsorption of Cr(VI) by LLAC adsorbent is multilayer with heterogeneous adsorption sites. The experimental data were well predicted by the pseudo-second-order kinetic model. Thus, it can be concluded that activated carbon from *Leucaena leucocephala* seed shell is highly effective for the removal of Cr(VI) from aqueous environment.

Open Access This article is distributed under the terms of the Creative Commons Attribution 4.0 International License (<http://creativecommons.org/licenses/by/4.0/>), which permits unrestricted use, distribution, and reproduction in any medium, provided you give appropriate credit to the original author(s) and the source, provide a link to the Creative Commons license, and indicate if changes were made.

References

- Akpan UG, Chubu JM, Olutoye MA (2015) Melon husk-based activated carbon for treatment of industrial wastewater. *Nigerian J Technol Res* 10(1):126–134
- Alias N, Zaini MAA, Kamaruddin MJ (2017) Roles of impregnation ratio of K_2CO_3 and NaOH in chemical activation of palm kernel shell. *J Appl Process Eng* 4(2):195–204
- Al-Othman Z, Ali R, Naushat M (2012) Hexavalent chromium removal from aqueous medium by activated carbon prepared from peanut shell: adsorption kinetics, equilibrium and thermodynamic studies. *Chem Eng J* 184:238–247
- Ani IJ, Okafor JO, Olutoye MA, Akpan UG (2015) Optimization of base oil regeneration from spent engine oil via solvent extraction. *Adv Res* 4(6):403–411
- Argun ME, Dursun S, Ozdemir C, Karatas M (2007) Heavy metal adsorption by modified oak sawdust: thermodynamic and kinetics. *J Hazard Mater* 14:77–85

- Atieh MA (2011) Removal of chromium (VI) from polluted water using carbon nanotubes supported with activated carbon. *Proc Environ Sci* 4:281–293
- Bohli T, Abdelmottaleb O, Nuria F, Isabel V (2015) Evaluation of an activated carbon from olive stones used as an adsorbent for heavy metal removal from aqueous solution. *C R Chim* 18:88–99
- Chiban M, Lehutu G, Sinan F, Carja G (2009) Arsenate removal by *Withania frutescens* plant from the south-western Morocco. *Environ Eng Manag J* 8:1377–1383
- Derdour K, Bouchelta C, Naser-Eddine AK, Medjram MS, Magri P (2018) Removal of Cr(VI) from aqueous solutions by using activated carbon supported iron catalysts as efficient adsorbents. *World J Eng* 15(1):3–13
- Dula T, Siraj K, Kitte SA (2014) Adsorption of hexavalent chromium from aqueous solution using chemically activated carbon prepared from locally available waste of bamboo (*Oxytenanthera abyssinica*). *ISRN Environ Chem* 1–9
- El Feel AA, Elmagboul AH (2016) Effect of planting density on *Leucaena leucocephala* woody stems production under arid dry climate. *Int J Environ Agric Res* 1–7
- Freundlich H (1906) Über die adsorption losungen (adsorption in solution). *Zeitschrift für Physikalische Chemie* 57:385–470
- Ganesan P, Kamaraj R, Sozhan G, Vasudevan S (2013) Oxidized multi walled carbon nanotube as adsorbent for the removal of manganese from aqueous solution. *Environ Sci Pollut Res* 20:987–996
- Garg UK, Kaur UK, Gary M, Sud O (2007) Removal of hexavalent chromium from aqueous solution by agricultural waste biomass. *J Hazard Mater* 140(1):60–68
- Ghasemi M, Ghoreyshi A, Younesi H (2015) Synthesis of a high characteristics activated carbon from walnut shell for the removal of Cr(VI) and Fe(II) from aqueous solution: single and binary solutes adsorption. *Iran J Chem Eng* 12:1–29
- Girgis BS, Temerk YM, Gadelrab MM, Abdullah ID (2007) X-ray diffraction patterns of activated carbons prepared under various conditions. *Carbon Sci* 8(2):95–100
- Giwa A, Akpan UG, Hameed BH (2012) Optimization of photocatalytic degradation of an anthraquinone dye using design of experiment. *J Eng Res* 17(3):20–31
- Gorzin F, Abadi MMBR (2017) Adsorption of Cr(VI) from aqueous solution by adsorbent prepared from paper mill sludge: kinetics and thermodynamic studies. *Adsorp Sci Technol* 0(0):1–21
- Gupta VK, Rastogi A, Naya KA (2010) Adsorption studies on the removal of hexavalent chromium from aqueous solution using a low cost fertilizer industry waste material. *J Colloid Interf Surf* 342:135–141
- Hameed BH, Krishna RR, Sata SA (2009) A novel agricultural waste adsorbent for the removal of cationic dye from aqueous solutions. *J Hazard Mater* 162:305–311
- Ho YS, McKay G (1998) Kinetic models for the sorption of dye from aqueous solution by wood. *Process Saf Environ Prot* 76:332–340
- Inglezakis VJ, Stylianou MA, Gkantouz D, Loizidou MD (2007) Removal of Pb(II) from aqueous solutions by using clinoptilolite and bentonite as adsorbents. *Desalination* 210:248–256
- Jorfi S, Ahmadi MJ, Pourfadakari S, Jaafarzadeh N, Soltani RDC, Akbari H (2017) Adsorption of Cr(VI) by natural clinoptilolite zeolite from aqueous solution: isotherms and kinetics. *Polish J Chem Technol* 19:106–114
- Jun LH, Tian LM, Li ZJ (2009) A kinetic study on the adsorption of Cr(VI) onto a natural material used as land fill liner. *Electron J Geotech Eng* 14:1–10
- Kamaraj R, Ganesan P, Vasudevan S (2015) Removal of lead from aqueous solutions by electrocoagulation: isotherm, kinetics and thermodynamic studies. *Int J Environ Sci Technol* 12:683–692
- Koby M (2004) Removal of Cr(VI) from aqueous solutions by adsorption onto hazelnut shell activated carbon: kinetic and equilibrium studies. *Biores Technol* 9(13):317–321
- Langergren S (1898) About the theory of so-called adsorption of soluble substances. *Kungliga Svenska Vetenskapsakademiers Handlingar* 24(4):1–39
- Lim SF, Lee AYW (2015) Kinetic study on removal of heavy metal ions from aqueous solution by using soil. *Environ Sci Pollut Res* 22:10144–10158
- Matlock MM, Howerton BS, Atwood DA (2001) Irreversible precipitation of mercury and lead. *J Hazard Mater* 84:72–83
- Mnif A, Bejaoui F, Mouelhi M, Hamrouni B (2017) Hexavalent chromium removal from model water and Cershock absorber factory effluent by nanofiltration and reverse osmosis membrane. *Int J Anal Chem* 3(1):1–10
- Mohammed-Ridha MJ, Ahmed AS, Raof NN (2017) Investigation of the thermodynamic, kinetic and equilibrium parameters of batch biosorption of Pb(II), Cu(II) and Ni(II) from aqueous phase using low cost biosorbent. *Al-Nahrain J Eng Sci (NJES)* 201:298–310
- Murugesan A, Vidhyadevi T, Kirupha SD, Ravikumar L, Sivanesan S (2013) Removal of chromium (VI) from aqueous solution using chemically modified corncob-activated carbon: equilibrium and kinetic studies. *Environ Prog Sustain Energy* 32:673–680
- Nurbas Nourbakhsh M, Kilicarslan S, Ilhan S, Ozdag H (2002) Biosorption of Cr⁺⁶, Pb⁺² and Cu⁺² ions in industrial waste water on *Bacillus* sp. *Chem Eng J* 85:351–355
- Oyedoh E, Ekwonu MC (2016) Experimental investigation on chromium (VI) using activated carbon resorcinol formaldehyde xerogels. *Acta Polytechnica* 56:373–379
- Radnia H, Ghoreyshi AA, Younesi H, Najafpour GO (2012) Adsorption of Fe(II) ions from aqueous phase by chitosan adsorbent: equilibrium, kinetic and thermodynamic studies. *Desalination Water Treat* 50(1–3):348–359
- Rahmani AR, Hossieni E, Poomohammadi A (2015) Removal of chromium (VI) from aqueous solution using electro-Fenton process. *Environ Process* 2(2):419–428
- Renuga DN, Manjusha K, Latitha P (2010) Removal of hexavalent chromium from aqueous solution using an eco-friendly activated carbon. *Adv Appl Sci Res* 1(3):247–254
- Selvi K, Pattabhi S, Kadirvelu K (2001) Removal of Cr(VI) from aqueous solution by adsorption onto activated carbon. *Bioresour Technol* 80(1):87–89
- Sing SP, Ma LQ, Hendry MJ (2006) Characterization of aqueous lead removal by phosphatic clay: equilibrium and kinetic studies. *J Hazard Mater B* 136:654–662
- Sugashini S, Begum KMMS (2015) Preparation of activated carbon from carbonized rice husk by ozone activation for Cr(VI) removal. *New Carbon Mater* 30(3):252–261
- Sumathi KMS, Mahimairaja S, Naidu R (2005) Use of low-cost biological waste and vermiculite for removal of chromium from tannery effluent. *Bioresour Technol* 96:309–316
- Vasudevan S, Lakshmi J (2011) Studies relating to an electrochemically assisted coagulation for the removal of chromium from water using zinc anode. *Water Sci Technol* 11(2):142–150
- Vunain E, Kenneth D, Biswick T (2017) Synthesis and characterization of low-cost activated carbon prepared from *Malawian baobab* fruit shells by H₃PO₄ activation for removal of Cu(II) ions: equilibrium and kinetics studies. *Appl Water Sci* 7:4301–4319
- Wang Y, Liu Q, Shu L, Miao M, Liu Y, Kong Q (2016) Removal of Cr(VI) from aqueous solution using Fe-modified activated carbon prepared from luffa sponge: kinetic, thermodynamic and isotherm studies. *Desalination Water Treat* 57(16):1–9
- Yu LJ, Shukla SS, Dorris KL, Shukla A, Margrave JL (2003) Adsorption of chromium from aqueous solutions by maple sawdust. *J Hazard Mater* 100:53–63